



HAL
open science

Impact of Endografting on the Thoracic Aortic Anatomy: Comparative Analysis of the Aortic Geometry before and after the Endograft Implantation

Marco Midulla, Ramiro Moreno, Anne Nègre-Salvayre, Franck Nicoud,
Jean-Pierre Pruvo, Stéphane Haulon, Hervé Rousseau

► To cite this version:

Marco Midulla, Ramiro Moreno, Anne Nègre-Salvayre, Franck Nicoud, Jean-Pierre Pruvo, et al.. Impact of Endografting on the Thoracic Aortic Anatomy: Comparative Analysis of the Aortic Geometry before and after the Endograft Implantation. *CardioVascular and Interventional Radiology*, 2014, 37 (1), pp.69-76. 10.1007/s00270-013-0601-7 . hal-00990700

HAL Id: hal-00990700

<https://hal.science/hal-00990700>

Submitted on 30 Oct 2018

HAL is a multi-disciplinary open access archive for the deposit and dissemination of scientific research documents, whether they are published or not. The documents may come from teaching and research institutions in France or abroad, or from public or private research centers.

L'archive ouverte pluridisciplinaire **HAL**, est destinée au dépôt et à la diffusion de documents scientifiques de niveau recherche, publiés ou non, émanant des établissements d'enseignement et de recherche français ou étrangers, des laboratoires publics ou privés.

Impact of Endografting on the Thoracic Aortic Anatomy: Comparative Analysis of the Aortic Geometry before and after the Endograft Implantation

Marco Midulla · Ramiro Moreno · Anne Negre-Salvayre ·
Franc Nicoud · Jean Pierre Pruvo · Stephan Haulon ·
Hervé Rousseau

Received: 20 December 2012 / Accepted: 30 January 2013 / Published online: 13 March 2013

Abstract

Purpose Although the widespread acceptance of thoracic endovascular aortic repair (TEVAR) as a first-line treatment option for a multitude of thoracic aortic diseases, little is known about the consequences of the device implantation on the native aortic anatomy. We propose a comparative analysis of the pre- and postoperative geometry on a clinical series of patients and discuss the potential clinical implications

Methods CT pre- and postoperative acquisitions of 30 consecutive patients treated by TEVAR for different pathologies (20 thoracic aortic aneurysms, 6 false aneurysms, 3 penetrating ulcers, 1 traumatic rupture) were used to model the vascular geometry. Pre- and postoperative geometries were compared for each patient by pairing and matching the 3D models. An implantation site was identified, and focal differences were detected and described.

Results Segmentation of the data sets was successfully performed for all 30 subjects. Geometry differences between the pre- and postoperative meshes were depicted

in 23 patients (76 %). Modifications at the upper implantation site were detected in 14 patients (47 %), and among them, the implantation site involved the arch (Z0–3) in 11 (78 %).

Conclusion Modeling the vascular geometry on the basis of imaging data offers an effective tool to perform patient-specific analysis of the vascular geometry before and after the treatment. Future studies will evaluate the consequences of these changes on the aortic function.

Keywords TEVAR · Stent graft · Thoracic aorta · Anatomy · Segmentation · Geometry

Introduction

Thoracic endovascular aortic repair (TEVAR) was presented to the medical community in the mid-1990s [1]; since then, technical evolutions of the devices and improvements in the treatment strategies have placed the endovascular repair as a first-line treatment option for a multitude of thoracic aortic diseases [2]. In spite of a

M. Midulla (✉) · J. P. Pruvo
Cardiovascular and Interventional Radiology, University
Hospital of Lille, Lille, France
e-mail: marco.midulla@chru-lille.fr

J. P. Pruvo
e-mail: jean-pierre.pruvo@chru-lille.fr

R. Moreno · H. Rousseau
Department of Radiology, Rangueil University Hospital,
Toulouse, France
e-mail: ramoroa@gmail.com

H. Rousseau
e-mail: rousseau.h@chu-toulouse.fr

R. Moreno · A. Negre-Salvayre · H. Rousseau
INSERM, UMR 1048, I2MC, Toulouse, France
e-mail: anne.negre-salvayre@inserm.fr

F. Nicoud
CNRS, UMR 5149 I3M, CC 051, University Montpellier II,
Montpellier, France
e-mail: franck.nicoud@univ-montp2.fr

S. Haulon
Department of Vascular Surgery, University Hospital of Lille,
Lille, France
e-mail: stephan.haulon@chru-lille.fr

multitude of clinical trials, institutional registers and case reports, little is known about the consequences of the device implantations on the native aortic status, in term of anatomy and function.

Actually, vascular anatomy has a crucial role for treatment planning and long-term outcomes of TEVAR. Automated methods for quantitative mapping of the aortic arch have been developed for TEVAR issues [3–5] on the basis of CT imaging. According to these experiences, the new approaches to the analysis of the vascular geometry by postprocessing techniques would help to improve preoperative planning and lead toward more patient-specific treatments. The significance of aortic anatomy (angulation, diameter) in achieving adequate stent graft fixation and seal [4, 6], and subsequently endoleak formation [7] has been extensively highlighted.

Besides this evidence, other investigators have focused on the role of the vascular geometry in the aortic hemodynamics by proposing applications of computational fluid dynamics (CFD) in order to provide realistic simulations of blood flow [8–11]. All these experiences have highlighted the importance of geometry variations of the aortic anatomy explaining subsequent hemodynamic properties of the blood flow.

We analyzed in a clinical series the modifications of the geometry induced by TEVAR on the aortic anatomy by comparing the 3D vascular volumes obtained by CT imaging-based modeling, and we discuss their potential clinical implications.

Materials and Methods

Population

Institutional database searches for TEVAR cases performed between January 2008 and January 2010 in two academic vascular centers were retrospectively reviewed. Thirty consecutive patients with good-quality imaging (24 men; median age 71 years, range 28–87 years) treated by TEVAR for different thoracic aortic pathologies (20 thoracic aortic aneurysms, 6 false aneurysms, 3 penetrating ulcers, 1 acute traumatic aortic rupture) were enrolled (Table 1). Patients with aortic dissections were excluded from this study because of the complexity of the vascular geometry in this aortic disease requiring separate manual segmentation of the true and false lumen.

Image Analysis and Geometry Reconstruction

A commercially available software for analysis of 3D data sets and mesh generation (Amira 5.0, TGS, Mercury

Table 1 Patient characteristics

Characteristic	Value
Age (year), median (range)	71 (28–87)
Gender	
Male	24 (80 %)
Female	6 (30 %)
Pathology	
Thoracic aortic aneurysm	20 (67 %)
False aneurysm	6 (20 %)
Penetrating ulcer	3 (10 %)
Acute traumatic aortic rupture	1 (3 %)
Proximal landing zone	
Z0	1 (3 %)
Z1	2 (6.5 %)
Z2	6 (20 %)
Z3	14 (47 %)
Z4	7 (23.5 %)

Computer Systems, USA), was used to analyze the CT images and segment the aortic volumes. Two senior radiologists with more than 5 years' experience in cardiovascular imaging (M.M. and H.R.) retrospectively reviewed the quality of acquisition.

Inclusion criterion was a good quality pre- and postoperative imaging available for the analysis. A minimum slice thickness of 3 mm with minimum interval reconstruction of 1 mm were considered mandatory for a good quality imaging. For each enrolled patient, a couple of DICOM data sets (pre- and posttreatment examinations) were archived. Aortic volume from each data set was segmented by the level-set technique [12] to generate the corresponding inner wall surface. The process included the whole aortic volume from the ascending to the descending aorta; the roots of the supra-aortic trunks were segmented along 3–4 cm above the origins. At the endograft implantation site, the in-stent surface was extracted. Segmentation of the landing zones was extended at least 3 cm proximal and 3 cm distal, respectively, to the proximal and distal sealing zones, as previously described for the analysis of aortic morphometry [4].

The 3D results of the modeling process were expressed and saved in stereolithography (.stl) format, which was suitable for both geometry analysis and further CFD applications.

Geometry Analysis

A patient-specific analysis of the geometry was performed by comparing the 3D meshes obtained for each patient from the native data sets (pre- and postoperative acquisitions). Both volumes were loaded on the software interface:

the transparency mode was used for plotting the preoperative volume, while for the postoperative view, either a shaded surface or a tetrahedral grid was adopted. This allowed overlapping of the two meshes and permitted recognition of the shape and contours of the two aortic volumes; the preoperative volume was shifted over the postoperative and 2D sections from the original postoperative data set could be overlaid in order to well depict the implantation site. Classical classification in zones 0–5 [13] was used to identify the landing zones. Analysis of the geometries was focused on the implantation zone: a good correspondence between the two meshes was defined as a same morphology of the vascular profiles when matching the two geometries. Focal differences were detected and described as focal narrowing of the mesh profiles, modified curvatures, skewness of the contours (Table 2).

Results

Image Analysis and Geometry Reconstruction

TEVAR was performed in 23 patients (76 %) with 1 stent graft and in 7 patients (24 %) with 2 stent grafts. Different devices were implanted (3 Talent, Medtronic, Minneapolis, MN, USA; 3 Relay, Bolton Medical, Sunrise, FL, USA; 11 Valiant, Medtronic; 20 Zenith TX 2, Cook, Bloomington, IN, USA). The proximal landing zone was at zone 0 (Z0) in 1 patient (3 %), at Z1 in 2 patients (6.5 %), at Z2 in 6 patients (20 %), at Z3 in 14 patients (47 %), and at Z4 in 7 patients (23.5 %). The distal landing zone was localized in the descending aorta (zones 4 or 5) in all patients but one (zone 3). Segmentation of the data sets was successfully performed for all 30 subjects. Thus, a total of 60 three-dimensional meshes were available for the comparative analysis. Each geometry reconstruction process required approximately 20 min.

Geometry Analysis

Comparative analysis of the pre- and postoperative geometries was possible for every patient. Good correspondence

Table 2 Comparative analysis

Characteristic	Proximal landing	In-stent zone	Distal landing
Geometry modification	14 (46 %) ^a	13 (43 %)	3 (10 %)
Modified curvature	5 (17 %)	4 (13 %)	0
Focal narrowing	7 (23 %)	3 (10 %)	0
Contour skewness	3 (10 %)	4 (13 %)	3 (10 %)

^a In patient 4, the postoperative geometry at the upper implantation site was characterized by a focal narrowing plus a sharp curvature of the arch (see text and Fig. 1)

between the pre- and postoperative vascular geometry was observed in 7 cases (24 %). Geometric differences between the pre- and postoperative meshes were depicted in 23 patients (76 %). In particular, modifications at the upper implantation site were detected in 14 patients (47 %), corresponding to 7 focal narrowing, 5 modifications of the arch curvature, and 3 cases of skewness of the vascular walls. Among them, the implantation site involved the arch (Z0–3) in 11 patients (78 %) (Figs. 1, 2, 3). Modifications of middle implantation site was observed in 6 cases: 4 changes of the aortic curvature (Fig. 4) and 2 focal narrowing of the aortic profile. A skewness of the contours characterized the postoperative geometry in 4 cases (Fig. 5). Modifications at the distal implantation site were observed in 4 patients (10 %) for slight irregularities of the contours. No stenosis or sharp tortuosity was observed.

Discussion

An institutional project dedicated to evaluate the impact of the endografting on the native thoracic aorta has been developed over the last 3 years at our institution. The present report, integrated into this project, is focused on the aortic anatomy. To our knowledge, it is the first patient-specific analysis on this topic on clinical series. Different authors have focused attention on the evaluation of the geometry of the thoracic aorta in relation to TEVAR issues, but none of these studies proposed a systematic comparative evaluation to initial anatomy for each patient [2, 4, 5, 14]. Some of these reports even proposed automated tools for quantitative characterization of the aortic morphology for subsequent improvements in device design, preoperative planning, and long-term outcomes [3]. The role of aortic tortuosity in relation with endoleak development has been assessed [4, 15], and some authors have recently suggested the significance of particular radiological configurations of the stent graft (“bird beak”) with the risk of type I and III endoleak [16]. These investigations evaluated CT or MR data from postimplantation acquisitions.

Here we present a patient-specific comparative analysis of the pre- and postoperative geometries focused on the implantation site. In nearly half of the patients (47 %), the geometry changed (stenosis and curvature changes) at the upper implantation zone. Interestingly, in 70 % of these, the proximal sealing was in the arch (Z1, Z2, and Z3). These findings confirm that the arch is a critical zone for the device delivery; according to previous reports, aortic arch tortuosity may affect late endoleak formation more than 6 months after TEVAR [15]. In Fig. 3, the aortic geometry has a coarctation aspect as a result of the stent graft morphology. This feature has already been described in patient-specific models of aortic dissections generated

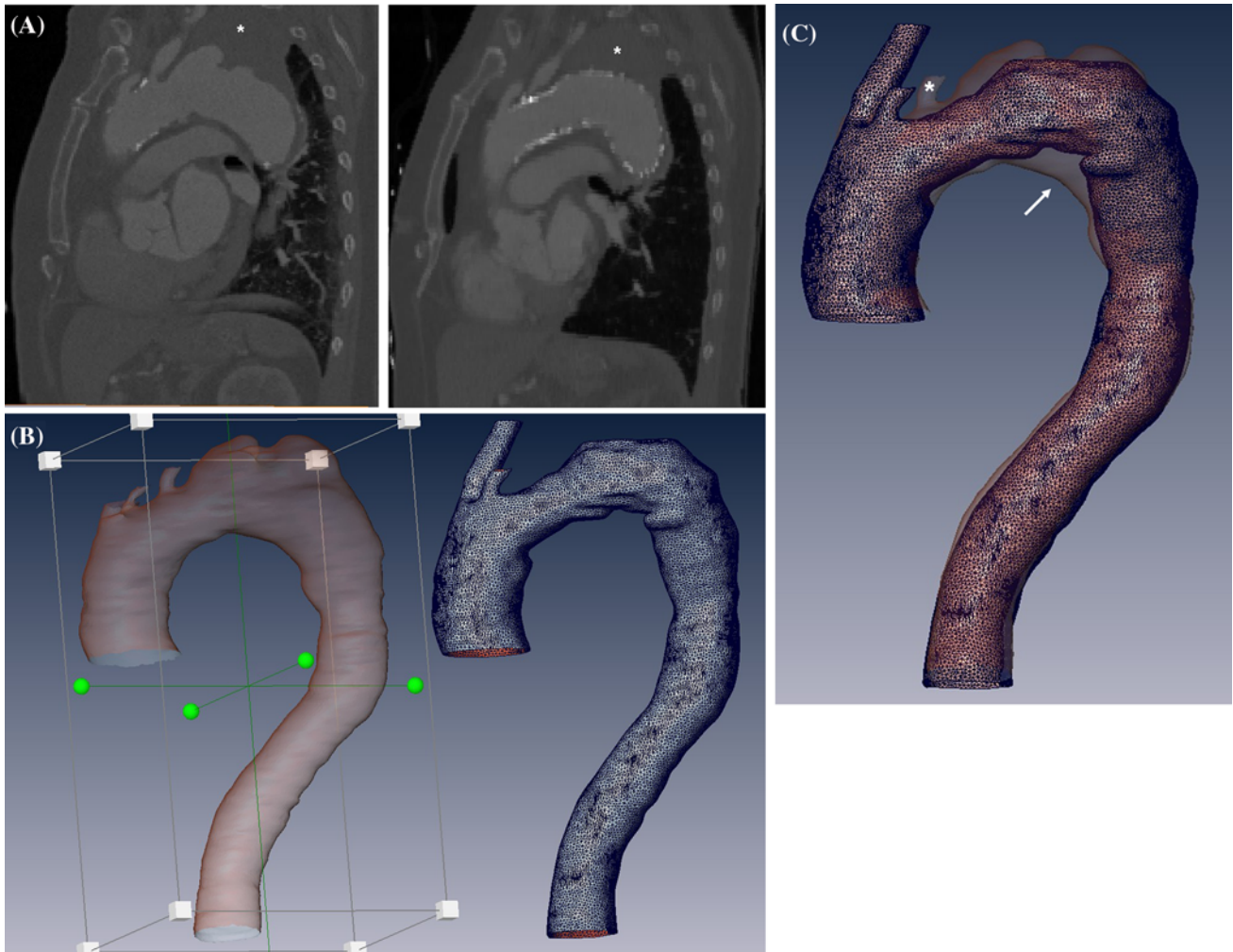


Fig. 1 Impact of TEVAR on the vascular geometry in a patient treated for a large thoracic aortic aneurysm of the arch and the proximal descending aorta, requiring endograft landing at Z2. **A** Multiplanar reconstructions (MPR) before (*left*) and after (*right*) the treatment. *Asterisks* show the lesion. **B** Reconstruction of the pre- (*left*, transparency mode) and postoperative (*right*, outlined mode) aortic geometries obtained by segmentation of the CT data sets.

C Overlapping of the 2 volumes confirmed left subclavian artery origin exclusion (*asterisk*) and revealed marked changes of the native anatomy after the device deployment, particularly related to the modification of aortic arch curvature. A sharp angulation is induced by the stent graft configuration at Z3 (*arrow*) and characterizes the postoperative mesh

for investigation of hemodynamics using CFD before and after thoracic aortic treatment [11].

The combination of MR and CT imaging with CFD for obtaining realistic simulations of the aortic flow has been largely described with both abdominal and thoracic EVAR [8–10, 17, 18]. In this methodological approach to functional imaging, geometry extraction plays a primary role in defining the fluid structure interactions to perform the calculations required to simulate the flow behavior. Virtual stent graft implantations or modifications of the pre- and postoperative geometries have been performed on the native meshes derived from the imaging data sets by different authors [9, 10, 19]. In our study, the whole set of 3D meshes (60 geometries), both before and after surgery, was obtained by segmentation of the native data sets. This

allowed for performing realistic assessments of the vascular geometry, particularly regarding the morphological changes induced by the endovascular treatment. Virtual stent graft implantation in the aortic arch has been performed by alignment of real grafts with projected 2D plane from CTA images [1, 5]. As shown in Figs. 1 and 3, our findings underline that the morphologic configuration of the device in the arch—as a result of its mechanical behavior during deployment as well as the intrinsic characteristics of the structure—is hardly predictable, and tremendous modifications of the aortic anatomy can occur after the implantation. In the next step of our project, the use of patient-specific geometries will allow to perform more realistic simulations of the aortic hemodynamics in combination with CFD. A comparative analysis of the



Fig. 2 Geometry analysis of a TEVAR for a descending thoracic aortic aneurysm with proximal landing zone at Z3. **A** Segmentations of the vascular volumes were performed systematically for the pre- (left) and postoperative (right) acquisitions. **B** Interface of the

software used for comparing the 2 geometries. The device implantation induced a sharp angulation of the postoperative anatomy (right) at the isthmic region

assessments on the pre- and postoperative status could be performed, using the entire data set, to investigate the functional implications of both major and even slight changes in the geometry (Fig. 5).

This pilot study has several limitations. First, it is just a first step toward assessing the impact of endografting on the native thoracic aorta. It is an observational report about

an early experience with the comparative analysis of pre- and postoperative 3D geometries. No quantitative assessment has been obtained because no automated tool for the quantification of the vascular geometry was available at the time we began the study. Different authors have proposed various approaches for the quantification of the aortic morphology, and in particular the arch. Most of them are

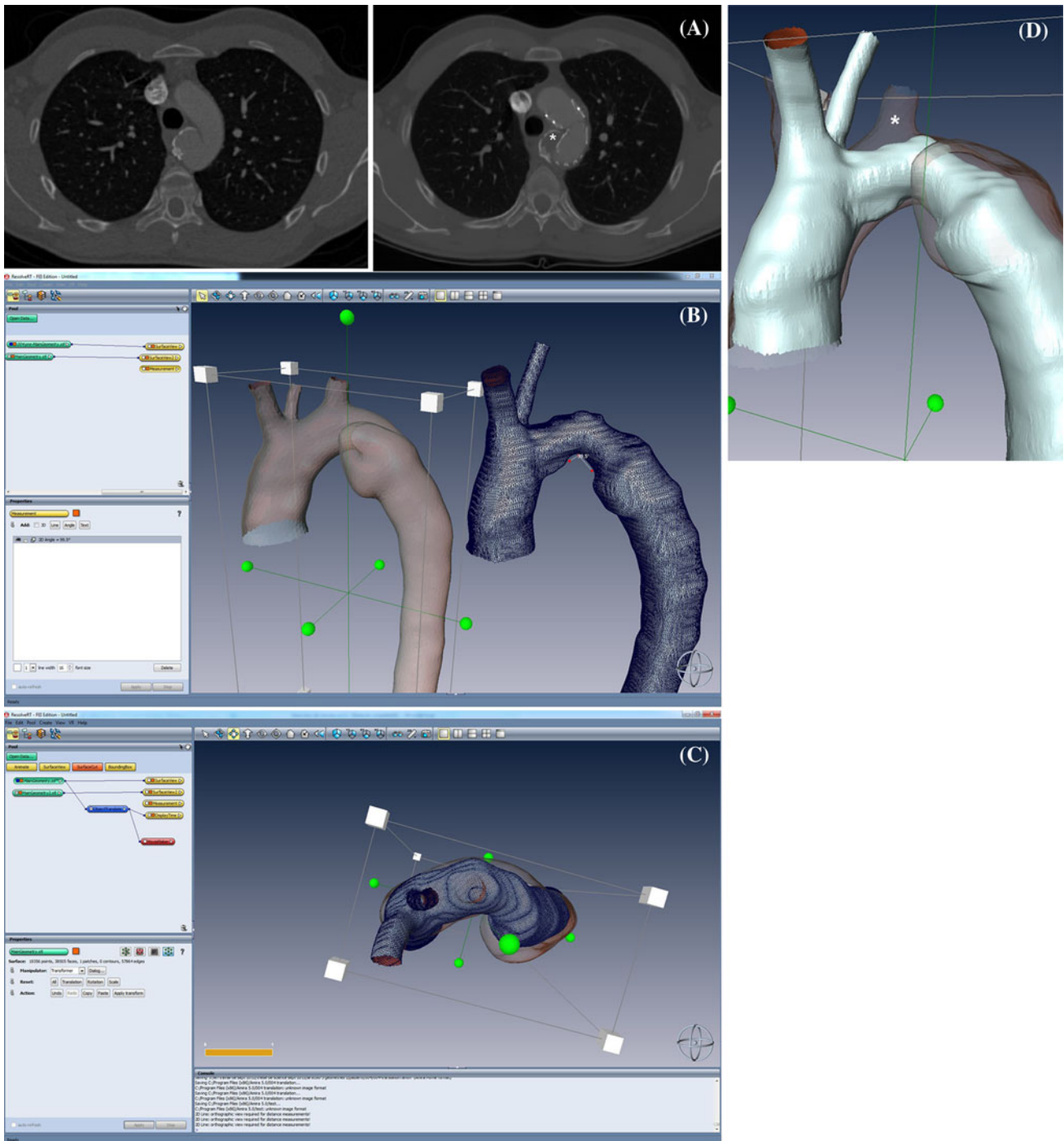


Fig. 3 Impact of TEVAR at the upper implantation site. **A** Axial images showing a false aneurysm of the isthmic region in a patient with past history of trauma. *Asterisk* indicates, on postoperative examination, the lesion excluded by the endograft. **B** The 2 geometries were modeled and **C** compared by matching the volumes.

D The use of the transparency mode for plotting the preoperative geometry allows to recognize the vascular contours of both meshes (the postoperative geometry is plotted as a *shaded surface*, *asterisk*). Modifications of the curvature with a focal narrowing were detected at the upper implantation site after the treatment

based on commercially available or in-house software that calculates the luminal centerline to extract diameters and different parameters related to vessel tortuosity, such as the tortuosity index [4], the curvature index, and the radius of

curvature [2, 14]. Visual assessment of tortuosity is subjective, and manual techniques for calculation of the radius and the angulation at the fixation zone do not reflect fully the complex and varied morphology of the diseased aorta

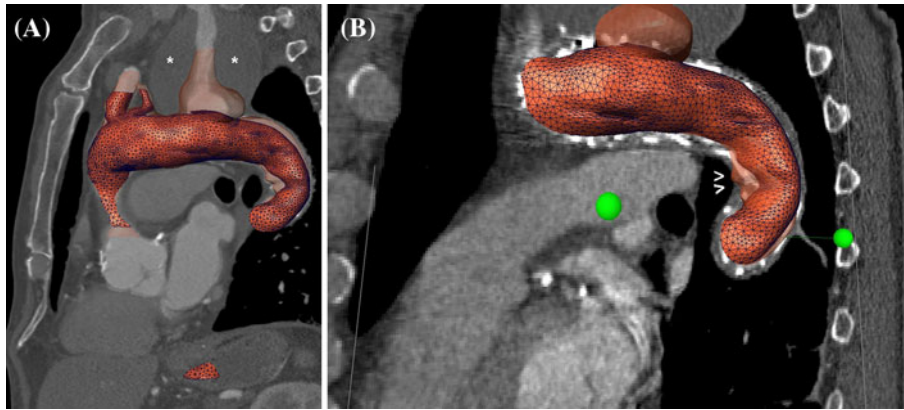
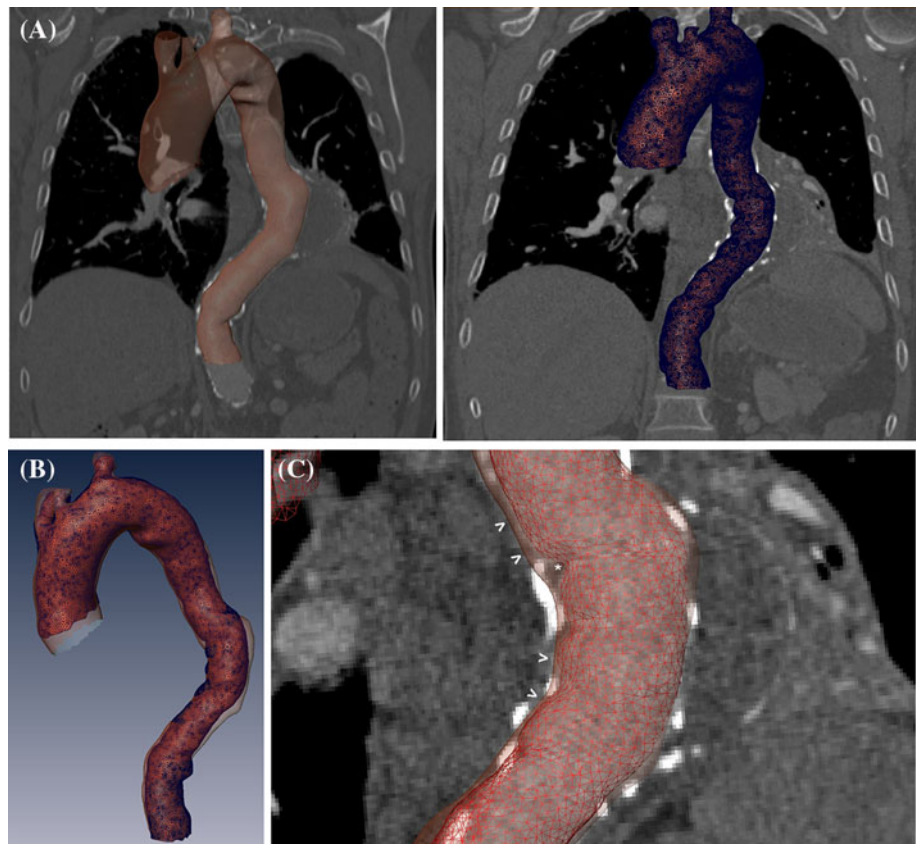


Fig. 4 Impact of thoracic endografting at the middle implantation site in a patient treated for a huge aneurysm of the left subclavian artery (LSA). **A** The 2 volumes (preoperative acquisition shown as transparent, postoperative acquisition plotted as a tetrahedral grid) are overlapped on a 2D sagittal section from the native preoperative

acquisition. The LSA is patent before the treatment with the thrombosed aneurysm around (*asterisks*). **B** A focal narrowing with sharp angulation (*arrowheads*) characterizes the postoperative vascular anatomy at the middle implantation site. 2D section from the postoperative acquisition shows the implanted stent graft

Fig. 5 Geometric analysis of a thoracic endografting for a descending thoracic aortic aneurysm: a case of skewness of the vascular profiles.

A Geometry reconstruction (using imaging data from the pre- and postoperative acquisitions, respectively shown as a transparent mesh on the *left* and a tetrahedral grid on the *right*). **B** Absence of focal narrowing or modification of the native curvature. **C** Inspection of the middle implantation site revealed a skewness of the contours of the postoperative geometry (*arrows*) which was related to in-stent hypodensities corresponding to parietal thrombus or graft infolding (*asterisk*). *Arrowheads* show the contours of the preoperative volume; postoperative geometry is plotted as a tetrahedral grid



[4, 20, 21]. The application of dedicated software could be proposed in next studies for quantitatively characterize the geometric changes and better assess the impact of endografting on the aortic anatomy.

The second limitation is the absence of a standard protocol for the CT acquisitions, especially for preoperative examinations, as patients were referred to our center by different institutions from a wide region. Patients were

enrolled consecutively when pre- and postoperative DICOM data with slice thickness of 3 mm and minimum interval reconstruction of 1 mm were available. These are limiting acquisition parameters already proposed for geometry reconstruction of the aortic anatomy in retrospective studies [17, 18]. A prospective approach with standard acquisition protocols defined for pre- and postoperative imaging would homogenize the geometry

extraction for future trials and eventual development of dedicated software for quantitative analysis of the geometry.

In conclusion, modeling the vascular geometry by means of imaging data offers an effective tool to perform patient-specific analysis of the vascular geometry before and after treatment. This preliminary comparative study demonstrates that the vascular anatomy can undergo radical changes after aortic endografting. The next step of our project will use the acquired set of reconstructed geometries to investigate the functional consequences of these modifications by a combined CT-CFD approach. A better understanding of the impact of endografting on the native thoracic aorta is crucial for future technical developments and clinical improvements in the management of pathology.

Acknowledgments Marco Midulla was supported during the development of his PhD project, of which this article is a part, by a grant from the French Society of Radiology (SFR). The entire project OCFIA is supported by the French National Agency for Research (ANR 07-CIS7-006-01).

Conflict of interest The authors declare that they have no conflict of interest.

References

1. Dake MD, Miller DC, Semba CP et al (1994) Transluminal placement of endovascular stent-grafts for the treatment of descending thoracic aortic aneurysms. *N Engl J Med* 331: 1729–1734
2. Nakatamari H, Ueda T, Ishioka F et al (2011) Discriminant analysis of native thoracic aortic curvature: risk prediction for endoleak formation after thoracic endovascular aortic repair. *J Vasc Interv Radiol* 22(974):979.e2
3. Rengier F, Worz S, Godinez WJ et al (2011) Development of in vivo quantitative geometric mapping of the aortic arch for advanced endovascular aortic repair: feasibility and preliminary results. *J Vasc Interv Radiol* 22:980–986
4. Ueda T, Takaoka H, Raman B et al (2011) Impact of quantitatively determined native thoracic aortic tortuosity on endoleak development after thoracic endovascular aortic repair. *AJR Am J Roentgenol* 197:W1140–W1146
5. Worz S, von Tengg-Kobligh H, Henninger V et al (2010) 3-D quantification of the aortic arch morphology in 3-D CTA data for endovascular aortic repair. *IEEE Trans Biomed Eng* 57: 2359–2368
6. Bortone AS, De Cillis E, D'Agostino D, de Luca Tuppiti Schinosa L (2004) Endovascular treatment of thoracic aortic disease: four years of experience. *Circulation* 110(11 suppl 1):II262–II267
7. Serag AR, Bergeron P, Mathieu X et al (2007) Identification of proximal landing zone limit for proper deployment of aortic arch stentgraft after supra-aortic great vessels transposition. *J Cardiovasc Surg (Torino)* 48:805–807
8. Midulla M, Moreno R, Baali A et al (2012) Haemodynamic imaging of thoracic stent-grafts by computational fluid dynamics (CFD): presentation of a patient-specific method combining magnetic resonance imaging and numerical simulations. *Eur Radiol* 22:2094–2102
9. Prasad A, To LK, Gorrepati ML et al (2011) Computational analysis of stresses acting on intermodular junctions in thoracic aortic endografts. *J Endovasc Ther* 18:559–568
10. Figueroa CA, Taylor CA, Chiou AJ et al (2009) Magnitude and direction of pulsatile displacement forces acting on thoracic aortic endografts. *J Endovasc Ther* 16:350–358
11. Tse KM, Chiu P, Lee HP, Ho P (2011) Investigation of hemodynamics in the development of dissecting aneurysm within patient-specific dissecting aneurismal aortas using computational fluid dynamics (CFD) simulations. *J Biomech* 44:827–836
12. Sethian JA (1999) Level set methods and fast marching methods: evolving interfaces in computational geometry, fluid mechanics, computer vision, and materials science. Cambridge University Press, New York
13. Fillinger MF, Greenberg RK, McKinsey JF, Chaikof EL (2010) Reporting standards for thoracic endovascular aortic repair (TEVAR). *J Vasc Surg* 52:1022–1033
14. Sze DY, van den Bosch MA, Dake MD et al (2009) Factors portending endoleak formation after thoracic aortic stent-graft repair of complicated aortic dissection. *Circ Cardiovasc Interv* 2:105–112
15. Czerny M, Grimm M, Zimpfer D et al (2007) Results after endovascular stent graft placement in atherosclerotic aneurysms involving the descending aorta. *Ann Thorac Surg* 83:450–455
16. Ueda T, Fleischmann D, Dake MD et al (2010) Incomplete endograft apposition to the aortic arch: bird-beak configuration increases risk of endoleak formation after thoracic endovascular aortic repair. *Radiology* 255:645–652
17. Molony DS, Kavanagh EG, Madhavan P et al (2010) A computational study of the magnitude and direction of migration forces in patient-specific abdominal aortic aneurysm stent-grafts. *Eur J Vasc Endovasc Surg* 40:332–339
18. Molony DS, Callanan A, Morris LG et al (2008) Geometrical enhancements for abdominal aortic stent-grafts. *J Endovasc Ther* 15:518–529
19. Filipovic N, Milasinovic D, Zdravkovic N et al (2011) Impact of aortic repair based on flow field computer simulation within the thoracic aorta. *Comput Methods Programs Biomed* 101:243–252
20. Sternbergh WC 3rd, Money SR, Greenberg RK, Chuter TA (2004) Influence of endograft oversizing on device migration, endoleak, aneurysm shrinkage, and aortic neck dilation: results from the Zenith Multicenter Trial. *J Vasc Surg* 39:20–26
21. Bowman JN, Silverberg D, Ellozy S et al (2009) The role of anatomic factors in predicting success of endovascular repair of thoracic aortic aneurysms. *Vasc Endovascular Surg* 44:101–104